

**Molecular components in  $P$ -wave charmed-strange mesons**Pablo G. Ortega,<sup>1,†</sup> Jorge Segovia,<sup>2,\*</sup> David R. Entem,<sup>3</sup> and Francisco Fernández<sup>3</sup><sup>1</sup>*CERN (European Organization for Nuclear Research), CH-1211 Geneva, Switzerland*<sup>2</sup>*Physik-Department, Technische Universität München,  
James-Frank-Straße 1, 85748 Garching, Germany*<sup>3</sup>*Grupo de Física Nuclear and Instituto Universitario de Física Fundamental y Matemáticas (IUFFyM),  
Universidad de Salamanca, E-37008 Salamanca, Spain*

(Received 26 July 2016; published 26 October 2016)

Results obtained by various experiments show that the  $D_{s0}^*(2317)$  and  $D_{s1}(2460)$  mesons are very narrow states located below the  $DK$  and  $D^*K$  thresholds, respectively. This is markedly in contrast with the expectations of naive quark models and heavy quark symmetry. Motivated by a recent lattice study which addresses the mass shifts of the  $c\bar{s}$  ground states with quantum numbers  $J^P = 0^+$  [ $D_{s0}^*(2317)$ ] and  $J^P = 1^+$  [ $D_{s1}(2460)$ ] due to their coupling with  $S$ -wave  $D^{(*)}K$  thresholds, we perform a similar analysis within a nonrelativistic constituent quark model in which quark-antiquark and meson-meson degrees of freedom are incorporated. The quark model has been applied to a wide range of hadronic observables, and thus the model parameters are completely constrained. The coupling between quark-antiquark and meson-meson Fock components is done using a  $^3P_0$  model in which its only free parameter  $\gamma$  has been elucidated, performing a global fit to the decay widths of mesons that belong to different quark sectors, from light to heavy. We observe that the coupling of the  $0^+$  ( $1^+$ ) meson sector to the  $DK$  ( $D^*K$ ) threshold is the key feature to simultaneously lower the masses of the corresponding  $D_{s0}^*(2317)$  and  $D_{s1}(2460)$  states predicted by the naive quark model and describe the  $D_{s1}(2536)$  meson as the  $1^+$  state of the  $j_q^P = 3/2^+$  doublet predicted by heavy quark symmetry, reproducing its strong decay properties. Our calculation allows us to introduce the coupling with the  $D$ -wave  $D^*K$  channel and the computation of the probabilities associated with the different Fock components of the physical state.

DOI: [10.1103/PhysRevD.94.074037](https://doi.org/10.1103/PhysRevD.94.074037)**I. INTRODUCTION**

The discovery in 2003 of the resonances  $D_{s0}^*(2317)$  ( $J^P = 0^+$ ) [1] and  $D_{s1}(2460)$  ( $1^+$ ) [2] yielded great interest among theorists and experimentalists due to their unexpected low masses and narrow widths. For instance, calculations based on quark models [3–8] and early lattice gauge theories [9–15] predicted for these states masses which were around 100 MeV above their respective  $DK$  and  $D^*K$  thresholds, whereas the experimental results lie 40 MeV below such thresholds.

Prior to the discovery of these two states, the heavy-light meson sectors were reasonably well understood in the  $m_Q \rightarrow \infty$  limit. In such a limit, heavy quark symmetry (HQS) holds [16]. The heavy quark acts as a static color source, its spin  $s_Q$  is decoupled from the total angular momentum of the light quark  $j_q$ , and they are separately

conserved. Then, the heavy-light mesons can be organized in doublets, each one corresponding to a particular value of  $j_q$  and parity. For the lowest  $P$ -wave charmed-strange mesons, HQS predicts two doublets, which are labeled by  $j_q^P = 1/2^+$  with  $J^P = 0^+, 1^+$  and by  $j_q^P = 3/2^+$  with  $J^P = 1^+, 2^+$ . The members of each doublet differ on the orientation of  $s_Q$  with respect to  $j_q$  and, in the heavy quark limit, are degenerated. Mass degeneracy is broken at order  $1/m_Q$ . Moreover, the strong decays of the  $D_{sJ}(j_q = 3/2)$  proceed only through  $D$  waves, while the  $D_{sJ}(j_q = 1/2)$  decays happen only through  $S$  waves [16]. The  $D$ -wave decay is suppressed by the barrier factor, which behaves as  $q^{2L+1}$ , where  $q$  is the relative momentum of the two decaying mesons. Therefore, states decaying through  $D$  waves are expected to be narrower than those decaying via  $S$  waves.

The  $D_{s0}^*(2317)$  and  $D_{s1}(2460)$  mesons are considered to be the members of the  $j_q^P = 1/2^+$  doublet, thus being almost degenerated and broad. However, neither the experimental values of their masses nor their empirical widths can be accommodated into the theoretical expectations.

These results led to many theoretical speculations about the nature of these resonances, ranging from conventional  $c\bar{s}$  states [17–19] to molecular or compact tetraquark interpretations [20–26]. More recently, a chiral unitary theory in

\*Corresponding author.

jorge.segovia@tum.de

†Present address: Instituto de Física Corpuscular (IFIC), CSIC-Universidad de Valencia, E-46071 Valencia, Spain.

*Published by the American Physical Society under the terms of the Creative Commons Attribution 3.0 License. Further distribution of this work must maintain attribution to the author(s) and the published article's title, journal citation, and DOI.*

coupled channels has explained that the  $D_{s_0}^*(2317)$  state is produced dynamically by means of the coupled channels  $DK$  and  $D_{s_1}\eta$  [27,28]. The analysis of the  $D_{s_0}^*(2317)$  meson's properties using other dynamical coupled-channel approaches for meson-meson in  $S$  waves can be found in Refs. [29–31]. In Ref. [32], a coupled-channel calculation of pseudo–scalar-vector mesons was performed in order to study the  $D_{s_1}(2460)$  and  $D_{s_1}(2536)$  states. It found masses of 2455 MeV and  $(2573.62 - i0.07)$  MeV, respectively. The second state couples mainly to  $DK^*$ ; however, the width is very small due to the fact that  $D^*K$  in  $D$  waves is not included. A molecular interpretation of the  $D_{s_2}^*(2573)$  state has been given in Ref. [33].

Certainly, quark models predict  $c\bar{s}$  ground states with quantum numbers  $J^P = 0^+$  and  $1^+$  that do not fit the experimental data. As the predictions of the quark models are roughly reasonable for other states in the charmed-strange sector [34,35], one must expect that the  $D_{s_0}^*(2317)$  and  $D_{s_1}(2460)$  resonances should be modifications of the genuine  $c\bar{s}$  states rather than new states out of the systematics of the quark model. On this respect, particularly relevant was the suggestion [36,37] that the coupling of the  $J^P = 0^+$  ( $1^+$ )  $c\bar{s}$  state to the  $DK$  ( $D^*K$ ) threshold plays an important dynamical role in lowering the bare mass to the observed value.

In a recent lattice study of the  $D_{s_0}^*(2317)$  meson [38], good agreement with the experimental mass is found when operators for  $DK$  scattering states are included. An extended version of the work performed in Ref. [38] was presented in Ref. [39]. They study the  $J^P = 0^+$ ,  $1^+$  and  $2^+$  charmed-strange mesons, incorporating the effect of nearby  $DK$  and  $D^*K$  thresholds. The  $D^*K$  threshold is incorporated only as an  $S$ -wave channel in the lattice QCD computations. However, the  $D$ -wave  $D^*K$  channel could play an important role in the  $1^+$   $c\bar{s}$  sector, in particular for the  $j_q^P = 3/2^+$   $D_{s_1}$  meson. Moreover, despite the significant progress made by lattice calculations incorporating  $DK$  and  $D^*K$  thresholds, no statement can be made about the probabilities of the different Fock components in the physical state.

The authors of Ref. [40] reanalyzed the lattice spectrum obtained in Refs. [38,39] using the auxiliary potential method and a reformulation (valid only for  $S$ -wave scattering amplitudes) of the Weinberg compositeness condition [41,42] to determine the amount of  $DK$  and  $D^*K$  components in the respective wave functions of  $D_{s_0}^*(2317)$  and  $D_{s_1}(2460)$  mesons. They found that the  $D_{s_0}^*(2317)$  meson is made by  $(72 \pm 13 \pm 5)\%$  of  $DK$  components, whereas the  $D_{s_1}(2460)$  meson contains  $(57 \pm 21 \pm 6)\%$  of  $D^*K$ .

In this paper, we study the low-lying  $P$ -wave charmed-strange mesons using a nonrelativistic constituent quark model in which quark-antiquark and meson-meson degrees of freedom are incorporated. The constituent quark model (CQM) was proposed in Ref. [43] (see Refs. [44,45] for reviews). This model successfully describes hadron phenomenology and hadronic reactions [46–48] and has

recently been applied to (non)conventional hadrons containing heavy quarks (see, for instance, Refs. [49–55]).

Within our approach, the coupling between the quark-antiquark and meson-meson sectors requires the creation of a light quark-antiquark pair. Therefore, the associated operator should be similar to the one which describes the open-flavor meson strong decays—namely, the  $^3P_0$  transition operator [56].

Our calculation allows us to introduce the coupling with the  $D$ -wave  $D^*K$  channel in the  $1^+$   $c\bar{s}$  sector and the computation of the probabilities associated with the different Fock components of the physical state, features which cannot be addressed nowadays by any other theoretical approach by itself.

This manuscript is arranged as follows: In Sec. II, we describe the main properties of our theoretical formalism, giving details about the approaches used to describe the quark-antiquark sector, the meson-meson sector and the coupling between them. Section III is devoted to presenting our results for the  $D_{s_0}^*(2317)$ ,  $D_{s_1}(2460)$ ,  $D_{s_1}(2536)$  and  $D_{s_2}^*(2573)$  mesons. We finish summarizing and giving some conclusions in Sec. IV.

## II. THEORETICAL FORMALISM

### A. Naive quark model

Constituent light quark masses and Goldstone-boson exchanges, which are consequences of dynamical chiral symmetry breaking in quantum chromodynamics (QCD), together with the perturbative one-gluon exchange (OGE) and a nonperturbative confining interaction, are the main pieces of our constituent quark model [43,45].

A simple Lagrangian invariant under chiral transformations can be written in the following form [57]:

$$\mathcal{L} = \bar{\psi}(i\not{\partial} - M(q^2)U^{\gamma_5})\psi, \quad (1)$$

where  $M(q^2)$  is the dynamical (constituent) quark mass and  $U^{\gamma_5} = e^{i\lambda_a \not{\partial}^{\gamma_5} \gamma_5 / f_\pi}$  is the matrix of Goldstone-boson fields that can be expanded as

$$U^{\gamma_5} = 1 + \frac{i}{f_\pi} \gamma^5 \lambda^a \pi^a - \frac{1}{2f_\pi^2} \pi^a \pi^a + \dots \quad (2)$$

The first term of the expansion generates the constituent quark mass, while the second gives rise to a one-boson exchange interaction between quarks. The main contribution of the third term comes from the two-pion exchange, which has been simulated by means of a scalar-meson exchange potential.

In the heavy quark sector, chiral symmetry is explicitly broken and Goldstone-boson exchanges do not appear. However, it constrains the model parameters through the light meson phenomenology [58] and provides a natural way to incorporate the pion exchange interaction in the molecular dynamics.

It is well known that multigluon exchanges produce an attractive linearly rising potential proportional to the distance between infinite-heavy quarks. However, sea quarks are also important ingredients of the strong interaction dynamics that contribute to the screening of the rising potential at low momenta and eventually to the breaking of the quark-antiquark binding string [59]. Our model tries to mimic this behavior using the following expression:

$$V_{\text{CON}}(\vec{r}) = [-a_c(1 - e^{-\mu_c r}) + \Delta](\vec{\lambda}_q^c \cdot \vec{\lambda}_{\bar{q}}^c), \quad (3)$$

where  $a_c$  and  $\mu_c$  are model parameters. At short distances this potential presents a linear behavior with an effective confinement strength,  $\sigma = -a_c\mu_c(\vec{\lambda}_i^c \cdot \vec{\lambda}_j^c)$ , while it becomes constant at large distances. This type of potential shows a threshold defined by

$$V_{\text{thr}} = \{-a_c + \Delta\}(\vec{\lambda}_i^c \cdot \vec{\lambda}_j^c). \quad (4)$$

No quark-antiquark bound states can be found for energies higher than this threshold. The system suffers a transition from a color string configuration between two static color sources into a pair of static mesons due to the breaking of the color flux tube and the most favored subsequent decay into hadrons.

The OGE potential is generated from the vertex Lagrangian

$$\mathcal{L}_{q\bar{q}g} = i\sqrt{4\pi\alpha_s}\bar{\psi}\gamma_\mu G_c^\mu \lambda^c \psi, \quad (5)$$

where  $\lambda^c$  are the  $SU(3)$  color matrices,  $G_c^\mu$  is the gluon field, and  $\alpha_s$  is the strong coupling constant. The scale dependence of  $\alpha_s$  can be found in e.g. Ref. [43]; it allows a consistent description of light, strange and heavy mesons.

To improve the description of the open-flavor mesons, we follow the proposal of Ref. [19] and include one-loop corrections to the OGE potential as derived by Gupta *et al.* [60]. These corrections show a spin-dependent term which affects only mesons with different flavor quarks. The net result is a quark-antiquark interaction that can be written as

$$V(\vec{r}_{ij}) = V_{\text{OGE}}(\vec{r}_{ij}) + V_{\text{CON}}(\vec{r}_{ij}) + V_{\text{OGE}}^{1\text{-loop}}(\vec{r}_{ij}), \quad (6)$$

where  $V_{\text{OGE}}$  and  $V_{\text{CON}}$  have been introduced above. The  $V_{\text{OGE}}^{1\text{-loop}}$  term is the one-loop correction to the OGE potential that contains central, tensor and spin-orbit contributions and whose particular expressions implemented in our model can be found in Ref. [61].

Explicit expressions for all the potentials and the values of the model parameters can be found in Ref. [43], updated in Ref. [62]. Meson eigenenergies and eigenstates are obtained by solving the Schrödinger equation using the Gaussian expansion method [63], which provides enough accuracy, and it simplifies the subsequent evaluation of the needed matrix elements.

Following Ref. [63], we employ Gaussian trial functions with ranges in geometric progression. This enables the optimization of ranges employing a small number of free parameters. Moreover, the geometric progression is dense at short distances, so that it enables the description of the dynamics mediated by short range potentials. The fast damping of the Gaussian tail does not represent an issue, since we can choose the maximal range to be much larger than the hadronic size.

## B. Coupled-channel quark model

The quark-antiquark bound state can be strongly influenced by nearby multiquark channels. In this work, we follow Ref. [64] to study this effect in the spectrum of the charmed-strange mesons, and thus we need to assume that the hadronic state is given by

$$|\Psi\rangle = \sum_\alpha c_\alpha |\psi_\alpha\rangle + \sum_\beta \chi_\beta(P) |\phi_A \phi_B \beta\rangle, \quad (7)$$

where  $|\psi_\alpha\rangle$  are  $c\bar{s}$  eigenstates of the two-body Hamiltonian,  $\phi_M$  are wave functions associated with the  $A$  and  $B$  mesons,  $|\phi_A \phi_B \beta\rangle$  is the two-meson state with  $\beta$  quantum numbers coupled to total  $J^P$  quantum numbers, and  $\chi_\beta(P)$  is the relative wave function between the two mesons in the molecule. When we solve the four-body problem, we also use the Gaussian expansion method (GEM) of the  $q\bar{q}$  wave functions obtained from the solution of the two-body problem. This procedure allows us to introduce in a variational way possible distortions of the two-body wave function within the molecule. To derive the meson-meson interaction from the  $q\bar{q}$  interaction, we use the resonating group method (RGM) [65].

The coupling between the quark-antiquark and meson-meson sectors requires the creation of a light quark pair. The operator associated with this process should describe also the open-flavor meson strong decays and is given by [66]

$$T = -\sqrt{3} \sum_{\mu,\nu} \int d^3 p_\mu d^3 p_\nu \delta^{(3)}(\vec{p}_\mu + \vec{p}_\nu) \frac{g_s}{2m_\mu} \sqrt{2^5 \pi} \times \left[ \mathcal{Y}_1\left(\frac{\vec{p}_\mu - \vec{p}_\nu}{2}\right) \otimes \left(\frac{1}{2}\right)_1 \right]_0 a_\mu^\dagger(\vec{p}_\mu) b_\nu^\dagger(\vec{p}_\nu), \quad (8)$$

where  $\mu(\nu)$  are the spin, flavor and color quantum numbers of the created quark (antiquark). The spin of the quark and antiquark is coupled to 1. The  $\mathcal{Y}_{lm}(\vec{p}) = p^l Y_{lm}(\hat{p})$  is the solid harmonic defined as a function of the spherical harmonic. We fix the relation of  $g_s$  with the dimensionless constant, giving the strength of the quark-antiquark pair creation from the vacuum as  $\gamma = g_s/2m$ , with  $m$  being the mass of the created quark (antiquark).

It is important to emphasize here that the  $^3P_0$  model depends on only one parameter, the strength  $\gamma$  of the decay interaction. Some attempts have been made to find possible

dependences of the vertex parameter  $\gamma$ ; see Ref. [67] and references therein. In Ref. [66] we performed a successful fit to the decay widths of the mesons which belong to the charmed, charmed-strange, hidden charm and hidden bottom sectors and elucidated the dependence on the mass scale of the  ${}^3P_0$  free parameter  $\gamma$ . Further details about the global fit can be found in Ref. [66]. The running of the strength  $\gamma$  of the  ${}^3P_0$  decay model is given by

$$\gamma(\mu) = \frac{\gamma_0}{\log(\frac{\mu}{\mu_0})}, \quad (9)$$

where  $\gamma_0$  and  $\mu_0$  are parameters, whereas  $\mu$  is the reduced mass of the quark-antiquark in the decaying meson. The value of  $\gamma$  that we are using in this work is the one corresponding to the charmed-strange sector:  $\gamma = 0.38$ .

From the operator in Eq. (8), we define the transition potential  $h_{\beta\alpha}(P)$  within the  ${}^3P_0$  model as [68]

$$\langle \phi_{M_1} \phi_{M_2} \beta | T | \psi_\alpha \rangle = P h_{\beta\alpha}(P) \delta^{(3)}(\vec{P}_{\text{cm}}), \quad (10)$$

where  $P$  is the relative momentum of the two-meson state.

The usual version of the  ${}^3P_0$  model gives vertices that are too hard, especially when we work at high momenta. Following the suggestion of Ref. [69], we use a momentum-dependent form factor to truncate the vertex as

$$h_{\beta\alpha}(P) \rightarrow h_{\beta\alpha}(P) \times e^{-\frac{P^2}{2\Lambda^2}}, \quad (11)$$

where  $\Lambda = 0.84$  GeV is the value used herein.

Adding the coupling with charmed-strange states, we end up with the coupled-channels equations

$$\begin{aligned} c_\alpha M_\alpha + \sum_\beta \int h_{\alpha\beta}(P) \chi_\beta(P) P^2 dP &= E c_\alpha, \\ \sum_\beta \int H_{\beta'\beta}(P', P) \chi_\beta(P) P^2 dP \\ + \sum_\alpha h_{\beta'\alpha}(P') c_\alpha &= E \chi_{\beta'}(P'), \end{aligned} \quad (12)$$

where  $M_\alpha$  are the masses of the bare  $c\bar{s}$  mesons and  $H_{\beta'\beta}$  is the RGM Hamiltonian for the two-meson states obtained from the  $q\bar{q}$  interaction. Solving the coupling with the  $c\bar{s}$  states, we arrive at a Schrödinger-type equation

$$\begin{aligned} \sum_\beta \int (H_{\beta'\beta}(P', P) + V_{\beta'\beta}^{\text{eff}}(P', P)) \\ \times \chi_\beta(P) P^2 dP &= E \chi_{\beta'}(P'), \end{aligned} \quad (13)$$

where

$$V_{\beta'\beta}^{\text{eff}}(P', P; E) = \sum_\alpha \frac{h_{\beta'\alpha}(P') h_{\alpha\beta}(P)}{E - M_\alpha}. \quad (14)$$

Finally, let us mention that this version of the coupled-channel quark model has been applied extensively to the study of XYZ states (see, for instance, Ref. [70]).

### III. RESULTS

Table I shows the masses of the low-lying  $P$ -wave charmed-strange mesons predicted by the naive quark model. One can see our results taking into account the one-gluon exchange potential ( $\alpha_s$ ) and including its one-loop corrections ( $\alpha_s^2$ ). The experimental data are taken from the Review of Particle Physics (RPP) [71].

The naive quark model predicts masses for the  $D_{s0}^*(2317)$  and  $D_{s1}(2460)$  mesons much higher than the experimental values. In fact, one can conclude from Table I that the  $j_q^P = 1/2^+$  and  $3/2^+$  doublets are predicted to be almost degenerated within the naive quark model. The state assigned to the  $D_{s0}^*(2317)$  meson is very sensitive to the one-loop corrections of the OGE potential, which bring its mass closer to the experimental one. This effect could explain part of its lower mass, but it is not enough, because our theoretical state is still above the  $DK$  threshold. The mass associated with the  $D_{s1}(2460)$  meson is roughly insensitive to the spin-dependent one-loop corrections of the OGE potential.

One can conclude from above that possible canonical  $c\bar{s}$  descriptions of the  $D_{s0}^*(2317)$  and  $D_{s1}(2460)$  mesons seem to fail when model parameters are kept to describe other quark sectors. From the conclusions of recent lattice-regularized QCD computations [38,39], the coupling of the  $J^P = 0^+ (1^+) c\bar{s}$  state to the  $DK$  ( $D^*K$ ) threshold appears as a possible mechanism to bring our theoretical masses to the experimental values.

HQS predicts that the members of the  $j_q^P = 1/2^+$  doublet [ $D_{s0}^*(2317)$  and  $D_{s1}(2460)$ ] couple equally to their respective  $DK$  and  $D^*K$  thresholds [72]. Moreover, because these states have the same mass in the limit  $m_Q \rightarrow \infty$ , the potentially generated mass shifts depend only on the energy difference between the bare  $c\bar{s}$  state and the open-flavored threshold. This would give a mass shift larger for the  $1^+ c\bar{s}$  state than for the  $0^+$  one, which is contrary to the experimental situation. The one-loop corrections of the OGE potential solve this issue and provide appropriate bare states whose mass shifts due to the continuum go in accordance with experiment.

TABLE I. Masses, in MeV, of the low-lying  $P$ -wave charmed-strange mesons predicted by the constituent quark model ( $\alpha_s$ ) and those including one-loop corrections to the one-gluon exchange potential ( $\alpha_s^2$ ). Experimental data are taken from Ref. [71].

State	$J^P$	Theoretical ( $\alpha_s$ )	Theoretical ( $\alpha_s^2$ )	Experimental
$D_{s0}^*(2317)$	$0^+$	2511	2383	$2318.0 \pm 1.0$
$D_{s1}(2460)$	$1^+$	2593	2570	$2459.6 \pm 0.9$
$D_{s1}(2536)$	$1^+$	2554	2560	$2535.18 \pm 0.24$
$D_{s2}^*(2573)$	$2^+$	2592	2609	$2571.9 \pm 0.8$

TABLE II. Values of  $m_{D_{s_0}^*(2317)} - m_{\overline{1S}}$ , in MeV, predicted by our quark model and lattice QCD [38], taking into account only quark-antiquark degrees of freedom and also coupling with the  $DK$  threshold. The value  $m_{D_{s_0}^*(2317)}$  is the mass of the  $D_{s_0}^*(2317)$  state, and  $m_{\overline{1S}} = 1/4(m_{D_s} + 3m_{D_s^*})$  is the spin-averaged ground-state mass. We compare with the experimental data taken from Ref. [71].

$D_{s_0}^*(2317)$	CQM	LQCD (1)	LQCD (2)	Experimental
$q\bar{q}$	309.0	$274.7 \pm 15.8$	$320.4 \pm 21.3$	$241.7 \pm 1.1$
$q\bar{q} + DK$	249.6	$254.4 \pm 4.9$	$245.0 \pm 15.5$	$241.7 \pm 1.1$
$V \rightarrow \infty$	...	$287.2 \pm 5.8$	$266.0 \pm 16.5$	$241.7 \pm 1.1$

### A. The dressed $D_{s_0}^*(2317)$ meson

Table II and Fig. 1 compare our results for the  $D_{s_0}^*(2317)$  mass with the lattice QCD study of Ref. [38] and with experiment [71]. Instead of the  $D_{s_0}^*(2317)$  itself, following the lattice study, we compare the values of  $m_{D_{s_0}^*(2317)} - m_{\overline{1S}}$ , where  $m_{\overline{1S}} = 1/4(m_{D_s} + 3m_{D_s^*})$  is the spin-averaged ground-state mass. Note that the lattice value of the  $D_{s_0}^*(2317)$  bound-state position in the infinite volume limit ( $V \rightarrow \infty$ ) is obtained by an analytical continuation of the scattering amplitude combined with Lüscher's finite volume method [38,39]. In Fig. 1, the dashed lines represent the threshold for  $DK$  in the different approaches, and the dotted lines are the thresholds for  $D^0K^+$  and  $D^+K^0$  in experiment.

The mass of the  $D_{s_0}^*(2317)$  state obtained using the naive quark model and without the one-loop spin corrections to the OGE potential is almost twice the experimental value,  $m_{D_{s_0}^*(2317)} - m_{\overline{1S}} = 437$  MeV. As we have discussed previously, the mass associated with the  $D_{s_0}^*(2317)$  state is

very sensitive to the  $\alpha_s^2$  corrections of the OGE potential. This effect brings down the  $m_{D_{s_0}^*(2317)} - m_{\overline{1S}}$  splitting to 309 MeV, which is now only 30% higher than the experimental figure. However, as one can see in Fig. 1, the hypothetical  $D_{s_0}^*(2317)$  would be above the  $DK$  threshold and thus would decay into this final channel in an  $S$  wave, making the state wider than the observed one. The mass shift due to the  $\alpha_s^2$  corrections allows that the  $0^+$  state can be close to the  $DK$  threshold. This makes the  $DK$  coupling a relevant dynamical mechanism in the formation of the  $D_{s_0}^*(2317)$  bound state. When we couple the  $0^+ c\bar{s}$  ground state with the  $DK$  threshold, the splitting  $m_{D_{s_0}^*(2317)} - m_{\overline{1S}} = 249.6$  MeV is in good agreement with experiment.

The lattice QCD simulation is performed on two very different ensembles of gauge configurations: ensemble 1, with two dynamical quarks, a pion mass of 266 MeV and a lattice size of  $16^3 \times 32$ ; and ensemble 2, with  $2+1$  dynamical quarks, a pion mass of 156 MeV and a lattice size of  $32^3 \times 64$ . One can see in Fig. 1 that the outcome from lattice simulations depends somewhat delicately on the pion mass even for very low masses. For the case of the largest pion mass and only quark-antiquark interpolators, unlike previous lattice simulations, the  $D_{s_0}^*$  appears below the  $DK$  threshold with a  $m_{D_{s_0}^*(2317)} - m_{\overline{1S}}$  in reasonable agreement with the experimental value; the inclusion of  $DK$  interpolators produces little effect in this case [see LQCD (1) results in Table II and Fig. 1]. In a near to physical light quark mass simulation [LQCD (2)], the  $D_{s_0}^*(2317)$  is above  $DK$  threshold when only quark-antiquark interpolators are included. In this case, the combination of  $q\bar{q}$  and  $DK$  lattice interpolating fields is crucial in order to get agreement with experiment. Finally,

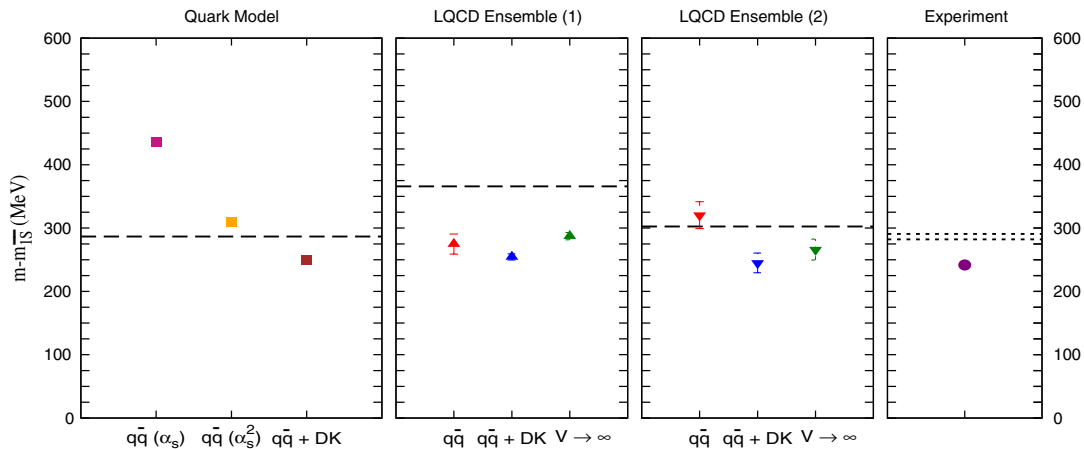


FIG. 1. Energy levels from the constituent quark model (CQM), from lattice QCD [38] using ensemble 1 and ensemble 2, and from experiment [71]. We show, for CQM results, the quark-antiquark value, taking into account the one-gluon exchange potential ( $\alpha_s$ ), including its one-loop corrections ( $\alpha_s^2$ ) and coupling with the  $DK$  threshold. For the lattice QCD results, in each ensemble, we show values with just a  $q\bar{q}$  interpolator basis and with a combined basis of  $q\bar{q}$  and  $DK$  interpolating fields. The value of the bound  $D_{s_0}^*(2317)$  state position in the infinite volume limit  $V \rightarrow \infty$  is obtained by an analytical continuation of the scattering amplitude combined with Lüscher's finite volume method. The dashed lines represent the threshold for  $DK$  in each approach, and the dotted lines are the thresholds for  $D^0K^+$  and  $D^+K^0$  in experiment.

TABLE III. Mass, in MeV, and probabilities of the different Fock components, in %, of the  $D_{s0}^*(2317)$  state.

State	Mass	$\mathcal{P}[q\bar{q}(^3P_0)]$	$\mathcal{P}[DK(S - \text{wave})]$
$D_{s0}^*(2317)$	2323.7	66.3%	33.7%

Table II and Fig. 1 show also the physical extrapolation of the  $m_{D_{s0}^*(2317)} - m_{\overline{15}}$  splitting in both ensembles. This value agrees with experiment and with our result when we incorporate the coupling of the  $DK$  threshold to the  $0^+ c\bar{s}$  state.

We turn now to discuss the probabilities of the different Fock components in the physical state. Lattice QCD studies [38,39] are only able to remark that both quark-antiquark and meson-meson lattice interpolating fields have non-vanishing overlaps with the physical state. Our wave function probabilities are given in Table III, which reflects that the  $D_{s0}^*(2317)$  meson is mostly of quark-antiquark nature. This is in agreement with the fact that lattice-regularized QCD computations observe this state even with only  $q\bar{q}$  interpolators (see Fig. 1). However, it is markedly in contrast with the 70% of  $DK$  obtained by Ref. [40] in the analysis of the lattice data of Refs. [38,39].

In our model, the probability of the  $DK$  state depends basically on three quantities: the bare meson mass, the  $^3P_0$  coupling constant and the residual  $DK$  interaction. Obviously, as neither of the three are observables, they can take different values depending on the dynamics, making the results, and hence the  $DK$  probability, model dependent.

In this paper we have constrained the mentioned parameters by reproducing other observable quantities like strong decays [66] (the  $^3P_0$  coupling constant), charmonium spectrum [62] (the bare mass) and  $NN$  and  $p\bar{p}$  interactions [73,74] (the  $DK$  residual interaction).

To check the uncertainties of the model, we have varied the value of the bare  $c\bar{s}$  mass and the  $^3P_0$  coupling  $\gamma$ , keeping the mass of the physical state to the experimental value. As expected in a model where the  $DK$  interaction is smaller than the effective interaction due to the coupling

with the  $c\bar{s}$  state, we obtain that the probability of the  $c\bar{s}$  component grows as the bare mass approaches the physical mass. To reproduce the scenario presented in Ref. [40], we would need a stronger residual  $DK$  interaction incompatible with the limits of the model. However, other dynamics are possible in quark models [75]; its analysis would be interesting in order to explore the possible convergence to the result of Ref. [40], but this task goes beyond the scope of the present work.

Finally, we have computed the scattering length associated with the physical  $D_{s0}^*(2317)$  state and obtain  $a(0^+) = -1.03$  fm. This number can be compared with the one estimated in Ref. [40]:  $-1.3 \pm 0.5$  fm; or with that from ensemble 2 of the lattice-regularized QCD computation [39]:  $-1.33 \pm 0.20$  fm. We conclude that our theoretical result is compatible, within errors, with those estimated by other approaches. The scattering length is sensitive to the amount of  $DK$  in the  $D_{s0}^*(2317)$  wave function. However, the uncertainties of the model do not allow us to compare in a precise way the molecular component of the different approaches.

## B. The dressed $D_{s1}(2460)$ and $D_{s1}(2536)$ mesons

Table IV and Fig. 2 compare our results for the mass of the first two  $J^P = 1^+$  charmed-strange states with the lattice QCD study of Ref. [39] and with experiment [71]. Instead of the masses themselves, following the lattice study, we compare their difference with respect to the spin-averaged ground-state mass,  $m_{\overline{15}} = 1/4(m_{D_s} + 3m_{D_s^*})$ . The lattice value of the  $D_{s1}(2460)$  bound-state position in the infinite volume limit ( $V \rightarrow \infty$ ) is obtained by an analytical continuation of the scattering amplitude combined with Lüscher's finite volume method. The mass of the  $D_{s1}(2536)$  meson is given directly from the lattice computations without resorting to the Lüscher method. In Fig. 2, the dashed lines represent the threshold for  $D^*K$  in the different approaches and the dotted lines are the thresholds for  $D^{*0}K^+$  and  $D^{*+}K^0$  in experiment.

 TABLE IV. Values of  $m_{D_{s1}(2460)} - m_{\overline{15}}$  and  $m_{D_{s1}(2536)} - m_{\overline{15}}$ , in MeV, predicted by our quark model and lattice QCD [39], taking into account only quark-antiquark degrees of freedom and also coupling with the  $D^*K$  threshold. The  $m_{D_{s1}(2460)}$  and  $m_{D_{s1}(2536)}$  are the masses of the  $D_{s1}(2460)$  and  $D_{s1}(2536)$  states, and  $m_{\overline{15}} = 1/4(m_{D_s} + 3m_{D_s^*})$  is the spin-averaged ground-state mass. We compare these with the experimental data taken from Ref. [71].

$D_{s1}(2460)$	CQM	LQCD (1)	LQCD (2)	Experimental
$q\bar{q}$	495.6	$383.3 \pm 4.5$	$398.4 \pm 12.5$	$383.3 \pm 1.0$
$q\bar{q} + D^*K(S)$	409.9	$377.4 \pm 4.2$	$392.0 \pm 11.0$	$383.3 \pm 1.0$
$V \rightarrow \infty$	...	$404.6 \pm 6.2$	$408.0 \pm 14.2$	$383.3 \pm 1.0$
$q\bar{q} + D^*K(S + D)$	409.8	...	...	$383.3 \pm 1.0$
$D_{s1}(2536)$	CQM	LQCD (1)	LQCD (2)	Experimental
$q\bar{q}$	486.0	$446.5 \pm 12.3$	$503.2 \pm 10.7$	$458.9 \pm 0.5$
$q\bar{q} + D^*K(S)$	488.0	$444.0 \pm 12.0$	$507.0 \pm 10.0$	$458.9 \pm 0.5$
$V \rightarrow \infty$	...	...	...	$458.9 \pm 0.5$
$q\bar{q} + D^*K(S + D)$	461.1	...	...	$458.9 \pm 0.5$

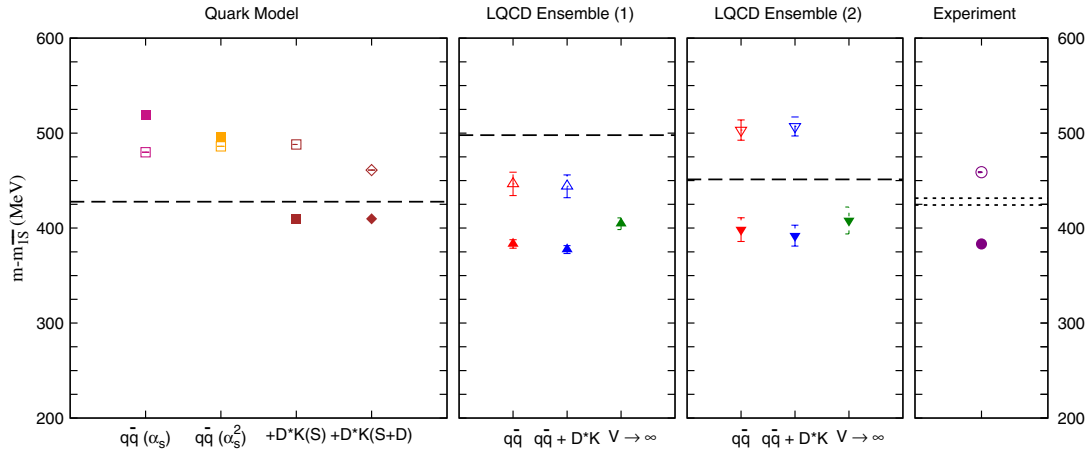


FIG. 2. Energy levels from the constituent quark model (CQM), from lattice QCD [39] using ensemble 1 and ensemble 2, and from experiment [71]. We show, for CQM results, the quark-antiquark value, taking into account the one-gluon exchange potential ( $\alpha_s$ ), including its one-loop corrections ( $\alpha_s^2$ ) and coupling with the  $D^*K$  threshold in  $S$  and  $D$  waves. For the lattice QCD results, in each case, we show values with just a  $q\bar{q}$  interpolator basis and with a combined basis of  $q\bar{q}$  and  $D^*K$  interpolating fields. Remember that in the lattice QCD computations the  $D^*K$  threshold is coupled only in an  $S$  wave. The value of the bound  $D_{s1}(2460)$  state position in the infinite volume limit  $V \rightarrow \infty$  is obtained by an analytical continuation of the scattering amplitude combined with Lüscher's finite volume method. This method has not been used for the  $D_{s1}(2536)$  meson. The dashed lines represent the threshold for  $D^*K$  in each approach, and the dotted lines are the thresholds for  $D^{*0}K^+$  and  $D^{*+}K^0$  in experiment.

The naive quark model predicts that the states corresponding to the  $D_{s1}(2460)$  and  $D_{s1}(2536)$  mesons are almost degenerated, with masses close to the experimentally observed mass of the  $D_{s1}(2536)$ . The inclusion of the one-loop corrections to the OGE potential does not improve the situation, making the splitting between the two states even smaller. Following lattice criteria, we first couple the  $D^*K$  threshold in an  $S$  wave with the two  $1^+ c\bar{s}$  states. One can see in Fig. 2 that the state associated with the  $D_{s1}(2460)$  meson goes down in the spectrum, and it is located below the  $D^*K$  threshold with a mass compatible with the experimental value. The state associated with the  $D_{s1}(2536)$  meson is almost insensitive to this coupling, because it is the  $J^P = 1^+$  member of the  $j_q = 3/2$  doublet predicted by HQS, and thus it couples mostly in a  $D$  wave to the  $D^*K$  threshold. Lattice QCD has not yet computed the coupling in the  $D$  wave of the  $D^*K$  threshold with the  $1^+ c\bar{s}$  sector. This coupling is trivially implemented in our approach. The state associated with the  $D_{s1}(2460)$  meson experiences a very small modification because it is almost the  $|1/2, 1^+\rangle$  eigenstate of HQS, whereas the state associated with  $D_{s1}(2536)$  meson suffers a moderate mass shift approaching the experimental value.

Some comments related with the lattice results are due here. The lowest level in both lattice ensembles is

associated with the physical state  $D_{s1}(2460)$ . This state is below the  $D^*K$  threshold in both lattice configurations (ensemble 1 and ensemble 2), and it is seen already when using only  $q\bar{q}$  interpolators. This observation should have important consequences in the interpretation of its compositeness. The level is downshifted by about 20 MeV (ensemble 1) or 30 MeV (ensemble 2) if  $D^*K$  interpolators are included [39]. The second state in both ensembles is identified with the  $D_{s1}(2536)$  meson. In ensemble 1, with the heavier pion, the state lies below the  $D^*K$  threshold, in strong disagreement with experimental observations. However, in the ensemble 2, the  $D_{s1}(2536)$  state appears above the  $D^*K$  threshold. For the two lattice configurations, the effect of coupling the  $D^*K$  threshold to both naive  $q\bar{q}$  states seems to be small (see Fig. 2). This is expected for the state associated with the  $D_{s1}(2536)$ , but not for the state associated with the  $D_{s1}(2460)$ , because the  $D^*K$  threshold is coupled only in the  $S$  wave. It is also found in lattice computations that the  $D_{s1}(2536)$  state is not seen if only  $D^*K$  interpolators are used.

Table V shows the probabilities of the different Fock components in the physical  $D_{s1}(2460)$  and  $D_{s1}(2536)$  states. When the  $D^*K$  threshold is coupled, the meson-meson

TABLE V. Mass and decay width, in MeV; and probabilities of the different Fock components, in %, of the  $D_{s1}(2460)$  and  $D_{s1}(2536)$  states. Results with and without coupling of the  $D$ -wave  $D^*K$  channel are listed.

State	Mass	Width	$\mathcal{P}[q\bar{q}(^1P_1)]$	$\mathcal{P}[q\bar{q}(^3P_1)]$	$\mathcal{P}[D^*K(S - \text{wave})]$	$\mathcal{P}[D^*K(D - \text{wave})]$
$D_{s1}(2460)$	2484.0	0.00	12.9%	32.8%	54.3%	...
$D_{s1}(2536)$	2562.1	0.22	34.4%	15.8%	49.8%	...
$D_{s1}(2460)$	2484.0	0.00	12.1%	33.6%	54.1%	0.2%
$D_{s1}(2536)$	2535.2	0.56	31.9%	14.5%	16.8%	36.8%

component is around 50% for both  $D_{s1}(2460)$  and  $D_{s1}(2536)$  mesons. This is in agreement with the fact that lattice calculations [39] find similar overlaps of the physical states with the quark-antiquark and meson-meson interpolators. Moreover, our prediction in this case is in agreement, within errors, with the one reported in Ref. [40]: the  $D_{s1}(2460)$  wave function has a probability of  $(57 \pm 21 \pm 6)\%$  for the  $S$ -wave  $D^*K$  component.

One may wonder why the molecular component is different in the  $D_{s0}^*(2317)$  and  $D_{s1}(2460)$  mesons, given that heavy quark symmetry predicts similar dynamics in both cases. Although HQS holds at the level of the interaction potential, it breaks due to the one-loop correction of the OGE potential, which is necessary to get the corresponding bare mass of the  $D_{s0}^*(2317)$ , and due to the different  $D^{(*)}K$  thresholds. In order to check this fact, we have disconnected the one-loop corrections and also artificially degenerated the respective meson-meson thresholds to avoid HQS breaking effects and observe that the  $DK$  and  $D^*K$  probabilities for the  $D_{s0}^*(2317)$  and  $D_{s1}(2460)$  mesons are very similar, around 60%.

It is also relevant to realize that the quark-antiquark component in the wave function of the  $D_{s1}(2536)$  meson holds quite well the  $^1P_1$  and  $^3P_1$  composition predicted by HQS. As pointed out in Ref. [76], this is crucial in order to have a very narrow state and describe well its decay properties. In Table VI we compare the results obtained in the present calculation with the updated ones of Ref. [76]<sup>1</sup> and the experimental results. The theoretical ratios, which pose very demanding constraints to the  $D_{s1}(2536)$  wave function, are compatible with experiment, indicating that our mixture for the  $D_{s1}(2536)$  wave function describes reasonably well the phenomenology of this state. Furthermore, the sophisticated coupled-channel study presented herein supports the more phenomenological one performed in Ref. [76].

As in the case of the  $D_{s0}^*(2317)$  meson, we have computed the scattering length associated with the physical  $D_{s1}(2460)$  state and obtain  $a(1^+) = -1.11$  fm. This number can be compared with the one estimated in Ref. [40]:  $-1.1 \pm 0.5$  fm; or with that from ensemble 2 of the lattice-regularized QCD computation [39]:  $-1.15 \pm 0.19$  fm (set 1) or  $-1.11 \pm 0.11$  fm (set 2). We conclude that our theoretical result is compatible, within errors, with those estimated by other approaches.

### C. The dressed $D_{s2}^*(2573)$ meson

The mass and total decay width of the  $D_{s2}^*(2573)$  meson are predicted well using naive quark models, and thus this

<sup>1</sup>The updated results of Ref. [76] quoted herein are slightly different from those of Ref. [76], since in this work we use the scale-dependent strength  $\gamma$  of the  $^3P_0$  model obtained in Ref. [66], which is very close to but not the same as the value used in Ref. [76].

TABLE VI. The total decay width,  $\Gamma$ , and the branching ratios  $R_1$ ,  $R_2$  and  $R_3$  defined in Ref. [76] for the present calculation. We compare these with the updated results of Ref. [76] (see text for details) and the experimental values reported by RPP [71].

	This work	Updated Ref. [76]	Experiment [71]
$\Gamma$ (MeV)	0.56	0.99	$0.92 \pm 0.03 \pm 0.04$
$R_1$	1.15	1.31	$1.18 \pm 0.16$
$R_2$	0.52	0.66	$0.72 \pm 0.05 \pm 0.01$
$R_3$ (%)	14.5	14.1	$3.27 \pm 0.18 \pm 0.37$

state is commonly expected to be a conventional charmed-strange meson. Moreover, the nearest  $DK$ -type thresholds are far enough to assume that they do not play an important role in the dynamical composition of the  $D_{s2}^*(2573)$  meson.

The same reasoning was followed by the lattice group [39], and only quark-antiquark operators in the configuration basis were used in the study of the  $D_{s2}^*(2573)$  meson. They also obtain a mass in qualitative agreement with experiment confirming that this state can be described well within the  $c\bar{s}$  picture.

Our predicted mass is shown in Table I; one can see our results taking into account the one-gluon exchange potential ( $\alpha_s$ ) and including its one-loop corrections ( $\alpha_s^2$ ). In both cases, our values are slightly higher than experiment but compatible.

We give in Table VII the partial and total strong decay widths of the  $D_{s2}^*(2573)$  meson. We show the absolute values in MeV and the branching fractions in percentages. One can see that the total decay width reported by PDG [71] is in excellent agreement with our result. The  $DK$  channel is clearly dominant with respect the other two possible decay channels,  $D^*K$  and  $D_s\eta$ . Therefore, in a coupled-channel calculation, the mass shift of the  $J^P = 2^+$  ground state would be an effect mainly driven by its coupling with the  $DK$  threshold. However, in order to do this, the  $D$  and  $K$  mesons should be in a relative  $D$  wave, and thus carrying extra momentum, which would imply a small mass shift.

Finally, we show in Fig. 3 the low-lying energy spectrum of the charmed-strange meson sector and compare it with those predicted by the two ensembles of lattice QCD.

TABLE VII. Open-flavor strong decay widths, in MeV, and branching fractions, in %, of the  $D_{s2}^*(2573)$  meson. Experimental data are taken from Ref. [71].

Channel	$\Gamma_{3P_0}$ (MeV)	$\mathcal{B}_{3P_0}$ (%)	$\Gamma_{\text{exp}}$ (MeV)
$D^+K^0$	8.02	42.95	...
$D^0K^+$	8.69	46.54	...
$D^{*+}K^0$	0.82	4.40	...
$D^{*0}K^+$	1.06	5.67	...
$D_s^+\eta$	0.08	0.44	...
Total	18.67	100	$17 \pm 4$

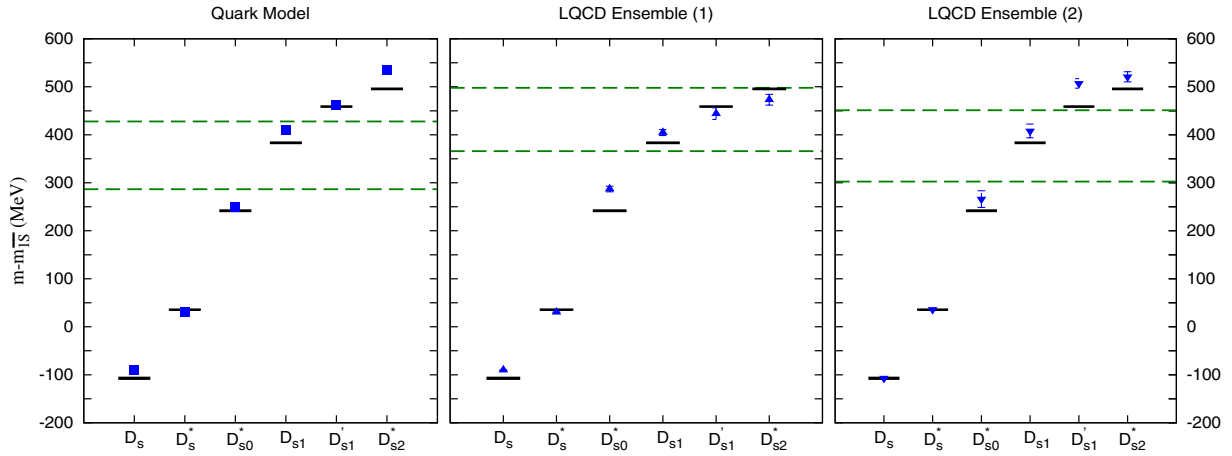


FIG. 3. Resulting  $D_s$  spectrum for all channels from CQM (squares), LQCD ensemble 1 (up-triangles) and LQCD ensemble 2 (down-triangles). The masses are presented with respect to the spin-averaged ground-state mass  $m_{15} = 1/4(m_{D_s} + 3m_{D_s^*})$ . The black solid lines correspond to experiment. The green dashed lines correspond to  $DK$  and  $D^*K$  thresholds in the respective approaches. Recall that the lattice values of the  $D_{s0}^*$ (2317) and  $D_{s1}$ (2460) bound-state positions in the infinite volume limit ( $V \rightarrow \infty$ ) are obtained by an analytical continuation of the scattering amplitude combined with Lüscher's finite volume method.

Leaving aside the spectrum obtained using ensemble 1, which has some features in strong disagreement with experimental observations, the spectrum predicted by our coupled-channel quark model and ensemble 2 of the lattice are in a global agreement and compare quite nicely with the experimental situation.

#### IV. EPILOGUE

We have performed a coupled-channel computation taking into account the  $D_{s0}^*$ (2317),  $D_{s1}$ (2460) and  $D_{s1}$ (2536) mesons and the  $DK$  and  $D^*K$  thresholds within the framework of a constituent quark model (CQM) whose parameters are largely constrained by hadron observables, from the light to the heavy quark sectors.

Our study has been motivated by the fact that recent lattice QCD computations need to incorporate explicitly meson-meson operators in their interpolator basis in order to obtain correct states for the physical  $D_{s0}^*$ (2317) and  $D_{s1}$ (2460) mesons. Our method allows us to introduce the coupling with the  $D$ -wave  $D^*K$  channel and the computation of the probabilities associated with the different Fock components of the physical state, features which cannot be addressed nowadays by lattice calculations.

The  $D_{s0}^*$ (2317) meson benefits most from the coupling of the  $DK$  threshold. The level assigned to it is much higher than the experimental value in the naive quark model. However, the one-loop corrections to the OGE potential bring down this level and locate it slightly above the  $DK$  threshold. This makes it so that the coupling with the nearby threshold acquires an important dynamical role. When coupling, the level is downshifted again towards the experimental mass of the  $D_{s0}^*$ (2317) meson, which is below the  $DK$  threshold. We predict a probability of 34% for the  $DK$  component of the  $D_{s0}^*$ (2317) wave function.

The naive quark model predicts that the states corresponding to the  $D_{s1}$ (2460) and  $D_{s1}$ (2536) are almost degenerated with masses close to the  $D_{s1}$ (2536) mass observed experimentally. The inclusion of the one-loop corrections to the OGE potential does not improve the situation, making the splitting between the two states even smaller. When the coupling with  $S$ - and  $D$ -wave  $D^*K$  threshold is performed, the states associated with the physical  $D_{s1}$ (2460) and  $D_{s1}$ (2536) mesons are in reasonable agreement with the experimental situation and lattice findings. We observe that the meson-meson component is around 50% for both  $D_{s1}$ (2460) and  $D_{s1}$ (2536) mesons. The  $D_{s1}$ (2536) meson appears as the  $|3/2, 1^+\rangle$  eigenstate of HQS, which is crucial to describing its decay properties.

The mass and total decay width of the  $D_{s2}^*$ (2573) meson are predicted reasonably well within our quark model approach taking into account only quark-antiquark degrees of freedom. We have calculated the partial decay widths of this state into open-flavored mesons. The  $DK$  channel is clearly dominant with respect to the other two possible decay channels,  $D^*K$  and  $D_s\eta$ . Therefore, in a coupled-channel calculation, the mass shift of the  $J^P = 2^+$  ground state would be an effect mainly driven by its coupling with the  $DK$  threshold. However, in order to do this, the  $D$  and  $K$  mesons should be in a relative  $D$  wave, thus carrying extra momentum, which would imply a small shift.

Finally, our spectrum of the low-lying charmed-strange mesons compares nicely with the most updated lattice QCD computation and with the experimental situation.

#### ACKNOWLEDGMENTS

We would like to thank M. Albaladejo, J. Nieves and D. Mohler for insightful comments. J. S. would like also to express his gratitude to N. Brambilla and A. Vairo for a careful

reading of the manuscript. This work has been partially funded by Ministerio de Ciencia y Tecnología under Contract No. FPA2013-47443-C2-2-P, by the Spanish Excellence Network on Hadronic Physics No. FIS2014-57026-REDT, and by the Junta de Castilla y León under Contract

No. SA041U16. P. G. O. acknowledges the financial support of the Spanish Ministerio de Economía y Competitividad and European FEDER funds under Contract No. FIS2014-51948-C2-1-P. J. S. acknowledges the financial support of the Alexander von Humboldt Foundation.

- 
- [1] B. Aubert *et al.* (BABAR Collaboration), *Phys. Rev. Lett.* **90**, 242001 (2003).
- [2] D. Besson *et al.* (CLEO Collaboration), *Phys. Rev. D* **68**, 032002 (2003); **75**, 119908(E) (2007).
- [3] S. Godfrey and R. Kokoski, *Phys. Rev. D* **43**, 1679 (1991).
- [4] J. Zeng, J. W. Van Orden, and W. Roberts, *Phys. Rev. D* **52**, 5229 (1995).
- [5] S. N. Gupta and J. M. Johnson, *Phys. Rev. D* **51**, 168 (1995).
- [6] D. Ebert, V. O. Galkin, and R. N. Faustov, *Phys. Rev. D* **57**, 5663 (1998); **59**, 019902(E) (1998).
- [7] T. A. Lahde, C. J. Nyfalt, and D. O. Riska, *Nucl. Phys.* **A674**, 141 (2000).
- [8] M. Di Pierro and E. Eichten, *Phys. Rev. D* **64**, 114004 (2001).
- [9] P. Boyle (UKQCD Collaboration), *Nucl. Phys. B, Proc. Suppl.* **53**, 398 (1997).
- [10] P. Boyle (UKQCD Collaboration), *Nucl. Phys. B, Proc. Suppl.* **63**, 314 (1998).
- [11] J. Hein, S. Collins, C. T. H. Davies, A. Ali Khan, H. Newton, C. Morningstar, J. Shigemitsu, and J. H. Sloan, *Phys. Rev. D* **62**, 074503 (2000).
- [12] R. Lewis and R. M. Woloshyn, *Phys. Rev. D* **62**, 114507 (2000).
- [13] G. S. Bali, *Phys. Rev. D* **68**, 071501 (2003).
- [14] M. di Pierro, A. X. El-Khadra, S. A. Gottlieb, A. S. Kronfeld, P. B. Mackenzie, D. P. Menscher, M. Okamoto, and J. N. Simone, *Nucl. Phys. B, Proc. Suppl.* **129**, 328 (2004).
- [15] A. Dougall, R. D. Kenway, C. M. Maynard, and C. McNeile (UKQCD Collaboration), *Phys. Lett. B* **569**, 41 (2003).
- [16] N. Isgur and M. B. Wise, *Phys. Rev. Lett.* **66**, 1130 (1991).
- [17] Fayyazuddin and Riazuddin, *Phys. Rev. D* **69**, 114008 (2004).
- [18] M. Sadzikowski, *Phys. Lett. B* **579**, 39 (2004).
- [19] O. Lakhina and E. S. Swanson, *Phys. Lett. B* **650**, 159 (2007).
- [20] T. Barnes, F. E. Close, and H. J. Lipkin, *Phys. Rev. D* **68**, 054006 (2003).
- [21] H. J. Lipkin, *Phys. Lett. B* **580**, 50 (2004).
- [22] P. Bicudo, *Nucl. Phys.* **A748**, 537 (2005).
- [23] A. P. Szczepaniak, *Phys. Lett. B* **567**, 23 (2003).
- [24] T. E. Browder, S. Pakvasa, and A. A. Petrov, *Phys. Lett. B* **578**, 365 (2004).
- [25] S. Nussinov, arXiv:hep-ph/0306187.
- [26] V. Dmitrasinovic, *Phys. Rev. Lett.* **94**, 162002 (2005).
- [27] A. Martinez Torres, L. R. Dai, C. Koren, D. Jido, and E. Oset, *Phys. Rev. D* **85**, 014027 (2012).
- [28] D. Gamermann, E. Oset, D. Strottman, and M. J. Vicente Vacas, *Phys. Rev. D* **76**, 074016 (2007).
- [29] M. Doring, J. Haidenbauer, U.-G. Meissner, and A. Rusetsky, *Eur. Phys. J. A* **47**, 163 (2011).
- [30] L. Liu, K. Orginos, F.-K. Guo, C. Hanhart, and U.-G. Meissner, *Phys. Rev. D* **87**, 014508 (2013).
- [31] Z.-H. Guo, U.-G. Meiner, and D.-L. Yao, *Phys. Rev. D* **92**, 094008 (2015).
- [32] D. Gamermann and E. Oset, *Eur. Phys. J. A* **33**, 119 (2007).
- [33] R. Molina, T. Branz, and E. Oset, *Phys. Rev. D* **82**, 014010 (2010).
- [34] J. Segovia, D. R. Entem, and F. Fernandez, *Phys. Rev. D* **91**, 094020 (2015).
- [35] Q.-T. Song, D.-Y. Chen, X. Liu, and T. Matsuki, *Phys. Rev. D* **91**, 054031 (2015).
- [36] E. van Beveren and G. Rupp, *Phys. Rev. Lett.* **91**, 012003 (2003).
- [37] E. van Beveren and G. Rupp, *Eur. Phys. J. C* **32**, 493 (2004).
- [38] D. Mohler, C. B. Lang, L. Leskovec, S. Prelovsek, and R. M. Woloshyn, *Phys. Rev. Lett.* **111**, 222001 (2013).
- [39] C. B. Lang, L. Leskovec, D. Mohler, S. Prelovsek, and R. M. Woloshyn, *Phys. Rev. D* **90**, 034510 (2014).
- [40] A. Martínez Torres, E. Oset, S. Prelovsek, and A. Ramos, *J. High Energy Phys.* **05** (2015) 153.
- [41] S. Weinberg, *Phys. Rev.* **137**, B672 (1965).
- [42] V. Baru, J. Haidenbauer, C. Hanhart, Yu. Kalashnikova, and A. E. Kudryavtsev, *Phys. Lett. B* **586**, 53 (2004).
- [43] J. Vijande, F. Fernandez, and A. Valcarce, *J. Phys. G* **31**, 481 (2005).
- [44] A. Valcarce, H. Garcilazo, F. Fernandez, and P. Gonzalez, *Rep. Prog. Phys.* **68**, 965 (2005).
- [45] J. Segovia, D. R. Entem, F. Fernandez, and E. Hernandez, *Int. J. Mod. Phys. E* **22**, 1330026 (2013).
- [46] F. Fernandez, A. Valcarce, P. Gonzalez, and V. Vento, *Phys. Lett. B* **287**, 35 (1992).
- [47] H. Garcilazo, A. Valcarce, and F. Fernandez, *Phys. Rev. C* **63**, 035207 (2001).
- [48] J. Vijande, H. Garcilazo, A. Valcarce, and F. Fernandez, *Phys. Rev. D* **70**, 054022 (2004).
- [49] J. Segovia, D. R. Entem, and F. Fernandez, *Phys. Rev. D* **83**, 114018 (2011).
- [50] P. G. Ortega, D. R. Entem, and F. Fernandez, *Phys. Lett. B* **718**, 1381 (2013).
- [51] J. Segovia, D. R. Entem, and F. Fernandez, *Nucl. Phys.* **A915**, 125 (2013).
- [52] P. G. Ortega, D. R. Entem, and F. Fernandez, *Phys. Rev. D* **90**, 114013 (2014).

- [53] P. G. Ortega, D. R. Entem, and F. Fernandez, *Phys. Lett. B* **729**, 24 (2014).
- [54] J. Segovia, D. R. Entem, and F. Fernandez, *Phys. Rev. D* **91**, 014002 (2015).
- [55] J. Segovia, P. G. Ortega, D. R. Entem, and F. Fernandez, *Phys. Rev. D* **93**, 074027 (2016).
- [56] A. Le Yaouanc, L. Oliver, O. Pene, and J. Raynal, *Phys. Rev. D* **8**, 2223 (1973).
- [57] D. Diakonov, *Prog. Part. Nucl. Phys.* **51**, 173 (2003).
- [58] J. Segovia, D. R. Entem, and F. Fernandez, *Phys. Lett. B* **662**, 33 (2008).
- [59] G. S. Bali, H. Neff, T. Duessel, T. Lippert, and K. Schilling (SESAM Collaboration), *Phys. Rev. D* **71**, 114513 (2005).
- [60] S. N. Gupta and S. F. Radford, *Phys. Rev. D* **24**, 2309 (1981).
- [61] J. Segovia, C. Albertus, E. Hernandez, F. Fernandez, and D. R. Entem, *Phys. Rev. D* **86**, 014010 (2012).
- [62] J. Segovia, A. M. Yasser, D. R. Entem, and F. Fernandez, *Phys. Rev. D* **78**, 114033 (2008).
- [63] E. Hiyama, Y. Kino, and M. Kamimura, *Prog. Part. Nucl. Phys.* **51**, 223 (2003).
- [64] P. G. Ortega, J. Segovia, D. R. Entem, and F. Fernandez, *Phys. Rev. D* **81**, 054023 (2010).
- [65] Y. C. Tang, M. Lemere, and D. R. Thompson, *Phys. Rep.* **47**, 167 (1978).
- [66] J. Segovia, D. R. Entem, and F. Fernandez, *Phys. Lett. B* **715**, 322 (2012).
- [67] J. Ferretti and E. Santopinto, *Phys. Rev. D* **90**, 094022 (2014).
- [68] Yu. S. Kalashnikova, *Phys. Rev. D* **72**, 034010 (2005).
- [69] D. Morel and S. Capstick, [arXiv:nucl-th/0204014](https://arxiv.org/abs/nucl-th/0204014).
- [70] P. G. Ortega, D. R. Entem, and F. Fernandez, *J. Phys. G* **40**, 065107 (2013).
- [71] K. A. Olive *et al.* (Particle Data Group), *Chin. Phys. C* **38**, 090001 (2014).
- [72] J. Nieves (private communication).
- [73] D. R. Entem, F. Fernandez, and A. Valcarce, *Phys. Rev. C* **62**, 034002 (2000).
- [74] D. R. Entem and F. Fernandez, *Phys. Rev. C* **73**, 045214 (2006).
- [75] L. R. Dai, Z. Y. Zhang, Y. W. Yu, and P. Wang, *Nucl. Phys. A* **727**, 321 (2003).
- [76] J. Segovia, A. M. Yasser, D. R. Entem, and F. Fernandez, *Phys. Rev. D* **80**, 054017 (2009).